ELSEVIER

Journal of Nuclear Materials 290–293 (2001) 381–388

journal of nuclear materials

www.elsevier.nl/locate/jnucmat

Hydrogen inventories in nuclear fusion devices

M. Mayer [a,*], V. Philipps [a], P. Wienhold [a], H.G. Esser [a], J. von Seggern [a], M. Rubel [b]

[a] *Forschungszentrum Jülich GmbH, Institut für Plasmaphysik, EURATOM Association, Trilateral Euregio Cluster, D-52425 Jülich, Germany*

[b] *Alfvén Laboratory, KTH Stockholm, Association EURATOM-NFR, 10405 Stockholm, Sweden*

Abstract

Hydrogen retention in tokamaks is due to implantation into plasma-facing materials and trapping in deposited layers. In the limiter tokamak TEXTOR-94 hydrogen-rich deposited layers with thicknesses up to 1 mm are observed on recessed parts of the limiters, areas perpendicular to the magnetic field in the scrape-off layer (SOL), neutralizer plates of the pumped limiter and inside the pumping ducts. In the divertor tokamak JET the main deposition is observed in the divertor, additional deposits are observed in the main chamber on the sides of the guard limiters. Codeposition of carbon ions with hydrogen is the major mechanism of layer growth at areas with direct plasma contact. At remote areas without direct plasma contact, sticking of neutral hydrocarbon radicals seems to play an important role for hydrogen trapping.

Keywords: Co-deposition; Deuterium inventory; Hydrogen retention

1. Introduction

The accumulation of tritium in the vessel wall materials of thermonuclear fusion devices is a major safety problem [1–4]. For ITER, a retention of 10–20 g T per 1000 s plasma pulse is predicted [4], resulting in unacceptably large amounts of accumulated T and in the need for frequent clean-up procedures.

Hydrogen is retained in the plasma facing first wall during a plasma discharge. This phenomenon has been called wall pumping. It is observed for stainless steel [5–7], beryllium [8,9] and carbon walls [10,11]. A large fraction of the retained hydrogen (typically $\gg 50\%$) is released from the walls after the discharge [9,12,13], resulting in a dynamic retention. Another fraction is retained permanently, leading to the accumulation of hydrogen in the vessel walls. Several mechanisms are responsible for hydrogen trapping [14]. By implantation of energetic hydrogen atoms or ions [15–17], by diffusion of implanted atoms into the bulk wall material [17–19], by adsorption of hydrogen gas on internal pore surfaces, and by codeposition of hydrogen with eroded Be, B or C atoms [20,21]. Trapped hydrogen atoms can be released from the vessel walls by ion induced detrapping [22,23] and thermal outgassing [23].

This paper focuses on the hydrogen inventory observed in TEXTOR-94. The similarities and differences with other experiments, namely JET and ASDEX-Upgrade, will be discussed.

2. TEXTOR-94

2.1. General

TEXTOR-94 is a medium-sized limiter tokamak (minor radius 0.46 m, major radius 1.75 m) and a typical pulse length of about 6 s. The total plasma exposed wall area is about 30 m^2, of which about 9.5 m^2 consist of carbon (toroidal ALT-II belt limiter, inner bumper

* Corresponding author. Permanent address: Max-Planck-Institut für Plasmaphysik, EURATOM Association, Boltzmannstr. 2, D-85748 Garching, Germany. Tel.: +49-89-3299-1639; fax: +49-89-3299-2279.

E-mail address: matej.mayer@ipp.mpg.de (M. Mayer).

0022-3115/01/$ - see front matter
PII: S0022-3115(00)00486-4

limiter, poloidal limiters, antenna limiters). The rest of the wall area, the so-called liner, is made of stainless steel (Inconel), covered with 50–100 nm amorphous hydrogenated boron (a-B:D) or silicon (a-Si:D) layers created during regular boronizations or siliconizations for wall conditioning. Liner and limiter temperatures were changed between 150°C and 350°C. Helium glow discharge cleaning (He-GDC) is applied occasionally. The TEXTOR-94 vessel is pumped through the ALT-II limiter with 8 turbomolecular pumps and additionally by the cryo panels of the neutral beam injector boxes.

2.2. Hydrogen fuel cycle and gas balance

Hydrogen wall pumping during ohmic discharges shows a complex behavior [24]. At the start of each discharge the wall pumping is high, but levels off as the discharge proceeds towards a steady-state value of roughly 1×10^{20} hydrogen atoms/s.

After a discharge hydrogen is released from the TEXTOR vessel walls. The time dependence of the release rate follows a uniform power law $\propto t^{-\alpha}$, with $\alpha = 0.70 \pm 0.05$. A similar power law was already observed at JET [9], and can be explained by thermal detrapping of trapped hydrogen atoms and volume recombination to hydrogen molecules [13]. Siliconized walls show a qualitatively similar behavior to boronized walls. The time dependence of the wall release rate and the exponent α are identical within the experimental uncertainties. The total amount of released hydrogen is both material- and temperature dependent.

A gas balance measurement quantifies the difference between the hydrogen gas input to the vessel and the hydrogen gas release from the vessel during typically one day of operation, i.e., it measures the amount of hydrogen atoms retained in the vessel during this time interval. Due to the dynamic behavior of the hydrogen release the gas balance is time dependent, but changes only slowly after sufficiently long time due to the decrease of the release rate by several orders of magnitude according to $t^{-\alpha}$.

The amount of hydrogen gas supplied into the TEXTOR-94 torus is determined with an accuracy of about 1%. For gas balance measurements the gas released between discharges is collected on the cryo panels of one neutral beam injector box, while all ALT-II limiter pumps are closed and the additional pumping capacity of the diagnostic system is only about 2%. A sequence of about 30 ohmic discharges was performed. The gas mixture condensed on the cryo panel is released by warming the panel to room temperature, the pressure is then measured with a baratron and the gas composition with 2 calibrated quadrupole mass spectrometers. Typically H_2 (2–9%), HD (23–28%), D_2 (50–60%), CD_3H together with HDO (mass 19, 1–3%) and CD_4 (1–2%) are observed. Additionally H_2O and mass 28 (mainly CO, but possibly also higher hydrocarbons) are measured. H atoms are always present in the walls due to the usual operation of TEXTOR-94 with neutral beam injection of H instead of D, with a typical H concentration in the plasma of about 10–15%. By operation in D the H is released by isotopic exchange from the walls, mainly as HD. The amounts of H_2 and H_2O, are not correlated with the amounts of HD and D_2, and therefore most likely do not originate from vessel wall areas with direct plasma contact, but have an additional source. One possibility may be outgassing from wall areas between the liner and the vacuum vessel wall.

The hydrogen gas balance of TEXTOR-94 for a full day of operation (about 8 h) is shown in Fig. 1 for boronized and siliconized wall conditions as a function of the liner temperature. All D atoms (from HD, D_2, CD_3H, CD_4) and additionally H atoms from HD and CD_3H were taken into account. A decrease of the wall temperature after long-term operation at higher temperatures increases the hydrogen retention, see data points *b* in Fig. 1. The decrease of the wall temperature from 620 to 420 K for one day increases the integral retention to nearly 60%. This is due to the smaller saturation concentration and higher outgassing at elevated temperatures, which makes additional trapping sites available if the temperature is decreased. In steady-state conditions, i.e., after long-term operation at a given temperature (see data points *a* in Fig. 1), the one day retention is considerably lower. A retention of about 11% at 420 K and around zero at 620 K is observed. The H-concentration in the released gas was about 13%-the retention for D only is therefore higher by the same amount.

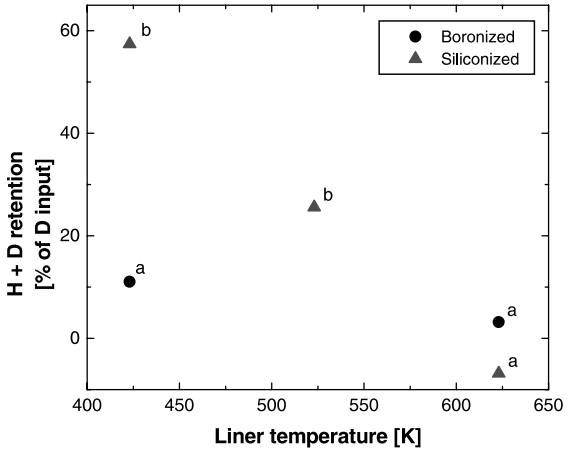

Fig. 1. Gas balance at TEXTOR-94 for boronized (circles) and siliconized (triangles) wall conditions. Data points labeled *a* were obtained after operating the machine for at least 30 days at the given liner temperature, while data points labeled *b* were obtained by operating the machine for 1 day at the given liner temperature after several weeks of operation at 630 K.

2.3. Hydrogen inventory

2.3.1. ALT-II limiter

A view of the toroidal ALT-II limiter is shown in Fig. 2. The black, curved area in the middle of the limiter (labeled *a*) is a net deposition zone, while the rest of the limiter surface is a net erosion area. It has been shown already, that the curvature of the tile surfaces and the ripple of the magnetic field result in a curvature of the power deposition pattern on the limiter surface [25].

Several ALT-II limiter tiles were analyzed with ion beam techniques and thermal desorption spectroscopy. A tile used from March to July 1997 for about 6300 discharge seconds showed redeposited layers with thicknesses of more than 12 μm, corresponding to an average growth rate of about 2 nm/s. On another tile (tile 20), used from January to August 1998 for 14100 discharge seconds, redeposited layers with thicknesses up to 50 μm are observed [26], corresponding to a maximum growth rate of about 3 nm/s. The redeposited layers consist mainly of C, originating most likely from the erosion-dominated areas on the ALT-II limiter. Additionally some B, Si and Inconel components (Ni, Fe, Cr) from erosion of the liner are observed. D is present at a level of about 0.1 D/C by codeposition with incident C ions. The D inventory of tile 20 reaches a maximum of 3.5×10^{19} atoms/cm^2 in the redeposition zone, while the D inventory in erosion-dominated areas is $3–7 \times 10^{17}$ atoms/cm^2, and $1–2 \times 10^{17}$ D-atoms/cm^2 are observed at the back of the tiles. The neighboring tile (tile 21) showed a very similar distribution of erosion/redeposition areas and the same D and B concentrations as tile 20. The observed, relatively low ratio of 0.1 D/C is due to loss of deuterium by temperature excursions during disruptions and long discharges (up to 10 s) with high power neutral beam heating. The redeposited layer has a low heat contact to the substrate and can heat up significantly. Additionally the D-inventory may be lowered by the presence of H, which is present at a level of about 1.1 H/D. This amount of H is larger by several orders of magnitude than expected from adsorption of H_2O at the very surface and may originate either from isotopic exchange with D or from additional uptake of H during storage in humid air. Such high levels of H were also observed previously at JET [27], but the detailed process of H-uptake is unknown.

The trapping of deuterium by codeposition on the ALT-II limiter is summarized in Table 1.

2.3.2. Liner

In general, the liner is a net erosion zone due to sputtering by high energetic neutral particles created in charge-exchange collisions [28–30]. The hydrogen inventory of the liner is therefore mainly determined by the inventory stored in a-B:D or a-Si:D layers created during boronizations or siliconizations. These layers are already saturated with D. The initial thickness of these coatings is about 80–100 nm, with a deuterium inventory of $1–2 \times 10^{17}$ atoms/cm^2. During plasma operation the layer thickness decreases by erosion, until the next coating is applied. The erosion rate depends on the toroidal and poloidal position [30]. In high erosion areas the coated layer may be completely eroded until the subsequent coating, while in low erosion areas only a small decrease of the initial layer thickness is observed. Long-term samples showed a D-inventory of 5×10^{15} atoms/cm^2 at high and 1×10^{17} atoms/cm^2 at low erosion areas after exposure for about 6 months [30]. Additionally H, with $H/D \geqslant 1$, is observed. The D inventory in the Inconel wall below the coating is small due to out-diffusion of hydrogen at the liner temperature of 570–620 K.

2.3.3. Wall areas perpendicular to the magnetic field in the SOL

Areas in the scrape-off layer (SOL) perpendicular to the magnetic field (='obstacles') are net deposition zones. This includes side faces of poloidal limiters, antenna protection limiters, screws, bolts, etc. The observed deposition during ohmic discharges on an aluminium collector probe is shown in Fig. 3 [31]. The deposited layer consists mainly of C. The maximum

Fig. 2. View of a segment of the ALT-II limiter, February 2000. Black region labeled *a*: net redeposition area.

Table 1
Trapping of D on different wall areas of TEXTOR-94. Growth rates of deposited layers, deuterium content, ratio of H–D, total area of the deposition zone and rate of deuterium trapping in this zone

	Growth rate (nm/s)	D/C ratio	H/D ratio	Area (m^2)	Retention rate (D-atoms/s)
ALT-II limiter	$\leqslant 3$	0.1	1.1	1	1.6×10^{19}
Obstacles in SOL	$\leqslant 12$	4×10^{-4}–0.4	[a]	0.2	1.2×10^{19}
Scoops, neutralizer	$\leqslant 20$	$\leqslant 7 \times 10^{-3}$	[a]	0.3	2×10^{18}
Pumping ducts	0.02	0.2	11	14	6×10^{18}
Total					3.6×10^{19}

[a] Not determined.

deposition rate of about 12 nm/s (about 1.2 μm after 107.7 s) is observed about 0.5 ± 0.3 cm outside the last closed flux surface (LCFS). The plasma density in the SOL decreases exponentially with a decay length of 10–20 mm [32], while the plasma temperature is $\leqslant$80 eV and changes more slowly (decay length 30–50 mm) than the plasma density [32]. The carbon concentration in the SOL is 2–4%. Therefore areas further away from the LCFS are subject to smaller incident carbon fluxes, resulting in a reduced layer growth rate. Areas closer to the LCFS, on the other hand, suffer a higher re-erosion by incident D ions, resulting in the maximum growth rate 0.5 cm outside the LCFS. Right at the LCFS net erosion is observed, resulting in a sharp transition between net erosion and net deposition areas. In discharges with additional neutral beam heating qualitatively a similar distribution of erosion/deposition regions is observed, but the net erosion region extends further out into the SOL until a radial position of about 48 cm.

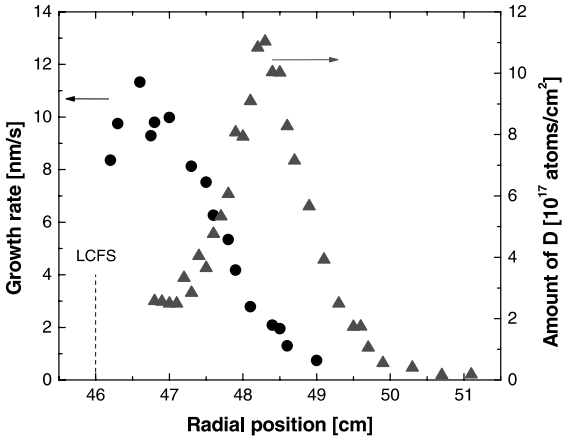

Fig. 3. Deposition on a collector probe perpendicular to the magnetic field in the scrape-off layer. Circles: layer growth rate. Triangles: deuterium inventory in the deposited layer. Dashed line: position of the last closed flux surface (LCFS). From [31].

The distribution of D shows a maximum about 2.3 cm outside the LCFS, with a D/C ratio close to 0.4. As in the case of the ALT-II limiter, D is trapped by co-deposition with incident carbon ions. Further outside the amount of D decreases due to the decrease of the codeposited layer thickness, while closer to the LCFS the incident power flux raises the surface temperatures, resulting in smaller D/C ratios. The tip of the sample shown in Fig. 3 reached surface temperatures $>$930 K.

The redeposited layers consist mainly of C, originating from the erosion-dominated areas of the ALT-II limiter. B is the major additional constituent at a level of 5–10%, traces of Fe, Cr and Ni ($<$1%) are observed. These elements originate from erosion of the liner [33,34].

Carbon deposition rates of 1–2 nm/s with a D/C ratio of $\sim$0.4 were already observed earlier two centimeters behind the LCFS [34–36]. On the side faces of a poloidal limiter carbon growth rates up to 4.5 nm/s and total layer thicknesses up to 150 μm were observed [33,37]. These layers showed a very low D/C ratio of 4×10^{-4} due to temperature excursions exceeding 1000°C during some discharges and were flaking off the substrate.

The trapping of deuterium by codeposition on obstacles in the SOL is summarized in Table 1. The uncertainty of the given numbers is large, due to the large variations of the D/C ratio and the layer growth rate with radial position.

2.3.4. Scoops and neutralizer plates of the ALT-II limiter pumps

The ALT-II limiter pumps are located at the bottom of the ALT-II limiter in a high flux area and consist of scoops and neutralizer plates made of carbon. After 3 years of operation from March 1997 until February 2000 (about 50 000 plasma seconds) deposited layers with thicknesses up to 1 mm (!) were observed (growth rate $\approx$ 20 nm/s), a view of a neutralizer plate is shown in Fig. 4. These are the thickest redeposited layers ever observed in TEXTOR. The layers were flaking off the substrate, thus producing dust particles. D is incorporated in these layers by codeposition, see Table 1. The

Fig. 4. Neutralizer plate of the ALT-II pumped limiter after 3 years of operation. Blade 8, February 2000. Original size: about 10×15 cm^2.

D/C-ratio was determined by ion beam analysis in the topmost 5 μm and is small, indicating high surface temperatures at least during some discharges.

2.3.5. Pumping ducts

Long-term samples were exposed in the pumping duct of ALT-II blade 7 from September 1999 until January 2000 (6250 plasma seconds) at a distance of about 1 m from the neutralizer plate. The temperature was about 350 K. After exposure soft hydrocarbon layers with a layer thickness of 130 nm were observed, corresponding to a growth rate of 0.02 nm/s. The refraction index of these layers was 1.52. They were mechanically soft and could be scratched with a paintbrush. The layers consist mainly of C, with only small traces of B and Si ($(B + Si)/C < 1\%$). O was present at a level of 0.03 O/C, most likely due to adsorption of water at the surface. The layers were hydrogen rich, with $(H + D)/C = 2.2$, which agrees well with the low refraction index. The majority of the trapped hydrogen was H, with $H/D = 11$.

Layer deposition at such remote areas must be accomplished by neutral particles, because only these can reach areas so far away from the plasma. The most likely candidates are hydrocarbon radicals like CD_3, C_2D, C_2D_3, as has been proposed by von Keudell et al. [38,39]. The H may originate either from isotopic exchange with D or by additional uptake of H, possibly from H_2O - any details of these processes are unknown.

The trapping of deuterium in the pumping ducts is summarized in Table 1. The uncertainty of the given numbers is large, mainly due to the poorly known layer thickness distribution. Also, it should be noted that the unknown origin of H is a crucial question. If isotopic exchange with D plays a role, then the original trapping of D may be up to 10 times larger than indicated in Table 1, thus becoming the dominant mechanism for D trapping.

2.3.6. Total

The deuterium retention rate on the different wall areas is summarized in Table 1. The majority of D is trapped in redeposition zones on the ALT-II limiter and obstacles perpendicular to the magnetic field in the SOL. Additionally a-C:D layers are formed on the scoops, neutralizer plates and pumping ducts of the limiter. The D is mainly codeposited with C ions, which originate from net erosion areas on the ALT-II limiter. The D content depends on the temperature history. In the pumping ducts the formation of much softer layers is observed, most likely by sticking of hydrocarbon radicals. The liner, being the largest surface area, is erosion dominated. Its D content is ruled by the amount of hydrogen contained in protective coatings (boronizations or siliconizations) and by implantation of charge-exchange deuterium.

The total D retention rate, as derived from wall analysis, is about 3.6×10^{19} D-atoms/s (Table 1). This agrees within the large error bars with the steady-state wall pumping rate of about 1×10^{20} D-atoms/s, which is observed at the end of a discharge, see Section 2.2 and Ref. [24].

3. JET

3.1. General

In contrast to TEXTOR-94 JET is a divertor experiment. The different JET divertors since 1994 were made of CFC tiles. Beryllium was used as divertor material only for a short time from April to June 1995. Poloidal guard limiters made of carbon are installed at the inner (about 10 m^2) and outer wall (about 11 m^2), the inner wall limiters are also used as start-up limiters during plasma build up. The vessel walls are made of Inconel (about 145 m^2). The remainder of the inner wall was cladded with carbon tiles in September 1996. Be evaporation is regularly applied for wall conditioning in order to reduce oxygen, resulting in a coverage of the outer wall with Be up to many μm thickness [40]. Some areas at the outer wall are shadowed from the evaporators by limiters, antennas etc. In these regions the Inconel wall still remains visible.

3.2. Gas balance

Gas balance measurements were performed for periods of 1 day, including overnight outgassing, by collecting the gas released between discharges on the cryo panels of the divertor pump. After regeneration to liquid nitrogen temperature, the gas was analyzed in the active gas handling system. Typically about 10% of the hydrogen input are retained, for details see [41,42].

3.3. Hydrogen inventory

3.3.1. Main chamber

The walls of the main chamber are net erosion areas due to sputtering by charge-exchange D atoms [28,43,44]. D is trapped by implantation at a level of about 1×10^{17} D-atoms/cm^2 in C at the inner wall [40], with a H/D ratio of 0.5–1. At the outer wall the D inventory increases up to 1×10^{18} D-atoms/cm^2 after 6 months [40]. The D is trapped in the evaporated Be layers deposited during wall conditioning at a D/Be ratio of 0.05–0.1. Additionally some carbon and metal impurities (Ni, Fe, Cr) are incorporated in these layers.

The carbon limiters at the inner and outer wall are eroded at the plasma facing front faces and show thick redeposited layers at their sides [44]. This behavior is very similar to TEXTOR-94 limiters. The layers consist mainly of C, with additional Be and traces of Fe, Ni and Cr. Only the very surface of these layers was analyzed, therefore only a lower limit of 3μm can be given for the thickness of these layers, though the total thickness may reach tens of μm. The D inventory was not analyzed. The limiters are a major source of carbon, at least during the start-up phase of each discharge, when the plasma is limited by the inner wall limiters [44]. It is assumed that these limiters are also an important carbon source during the divertor phase [27,44], but from current knowledge this cannot be quantified. Any other obstacles in the main chamber SOL were not analyzed, but are expected to be additional redeposition areas comparable to the findings at TEXTOR, see Section 2.3.3.

3.3.2. Divertor

The D and T inventories of the different JET divertors were analyzed in more detail than other wall areas [27,45–48]. The Mark I divertor was used from April 1994 to March 1995 with CFC tiles and from April to June 1995 with Be tiles. The Mark I had large gaps between the tiles (about 15% of the total divertor surface were gaps). Redeposited layers consisting mainly of C ($\geqslant 80\%$) with about 5–10% Be, 5–10% N + O and traces of Ni, Fe and Cr, were observed mainly in areas toroidally shadowed by adjacent tiles (about 30–50% of each tile surface) [46], and in the inner divertor corner [43,44]. The amount of D trapped in the Mark I C tiles was about 5×10^{17} atoms/cm^2 in the plasma exposed surfaces, and $>5 \times 10^{18}$ D-atoms/cm^2 in the shadow [46], with about 0.2 D/C. Additionally about the same amount of H was observed. The layers are most likely formed by codeposition of D with C ions. The C may originate partly from the plasma exposed part of the divertor tiles, and partly from the main chamber carbon limiters. This is suggested by the fact that even with Be divertor tiles large amounts of redeposited C were observed.

The Mark IIA divertor, used from April 1996 until February 1998, and the Mark IIGB divertor, which is used since June 1998, have a smaller number of much larger tiles than the Mark I, and much smaller gaps between tiles. Pumping is accomplished through gaps between floor and side wall modules at the inner and outer corners. Water-cooled louvres are located behind these gaps for protection of the cryo-pumps. Massive deposits ($>3 \times 10^{19}$ D-atoms/cm^2) are observed on the tiles close to the gaps and on the louvres [27,47,48]. The deposits tend to flake off the substrate. The D/C ratio is high (about 0.8), indicating soft a-C:D films. The subdivertor areas were not analyzed yet, but may contain additional deposits. This is suggested by the observation of deposited thick layers at the back side of divertor tiles in ASDEX-Upgrade [49].

Because the louvres have no direct plasma contact, a mechanism different from codeposition of D and C ions must be responsible for the observed deposits. Deposition during ELMs, enhanced erosion of redeposited layers (by a factor of about 10) and layer growth by sticking of neutral hydrocarbon radicals released by thermal decomposition of soft hydrocarbon films [38,39] have been proposed. A major influence of ELMs seems unlikely, as is shown by gas balance measurements. The amounts of trapped hydrogen during ELMy H-mode and ELM-free L-mode are identical within the experimental error bars. The observation of deposited layers in the pumping ducts of TEXTOR-94 (Section 2.3.5) and in the sub-divertor area of ASDEX-Upgrade [49] show clearly a contribution of neutral particles. Because these wall areas can be accessed only after several wall collisions, the sticking coefficient must be below 1. This makes a contribution of hydrocarbon radicals to layer growth likely.

4. Conclusions

Both in limiter and divertor tokamaks the walls of the main chamber and the plasma exposed limiter faces are net erosion areas. Additionally the divertor strike points may be net erosion areas, though they may change to net deposition areas if the plasma temperature in the divertor is sufficiently low. The amount of hydrogen present in these areas is determined by wall conditioning techniques (boronization, siliconization) and hydrogen implantation. From the viewpoint of T inventory these areas are not critical, at least as long the implanted hydrogen does not diffuse into the bulk material and gets trapped there.

Eroded material is redeposited on more recessed parts of limiters, areas perpendicular to the magnetic field in the SOL and divertor areas in the shadow. These redeposited layers consist mainly of C, with additional constituents like B, Si, Ni, Cr or Fe eroded from other

wall areas, and may contain hydrogen up to 0.4 D/C due to codeposition. The amount of trapped hydrogen depends on the temperature history of the samples, and may be as low as 10^{-4} D/C at areas where the surface temperature exceeds 1000°C. Due to the high fluxes of C the layer growth rate is of the order of several nm/s, and layer thicknesses up to 1 mm are observed. If the layer thickness exceeds several μm, the layers begin to flake partly off the substrate, resulting in the formation of dust particles.

Additional deposited layers are observed on areas far away from the plasma, like water-cooled louvres (JET), inside pumping ducts (TEXTOR-94) and sub-divertor areas (ASDEX-Upgrade). These redeposited layers consist mainly of C. They are mechanically soft, and may contain larger amounts of hydrogen up to ≈ 2 $(H + D)/C$. The most likely layer formation mechanism is sticking of hydrocarbon radicals. Again, thicker layers tend to flake partly off the substrate.

From the viewpoint of tritium inventory the use of carbon has severe disadvantages. It is able to trap nearly unlimited amounts of hydrogen in amorphous hydrocarbon layers, the hydrogen can be released only at high temperatures, and these layers can be formed at remote areas hard to access due to hydrocarbon radical sticking. Though the use of carbon is beneficial in today's fusion experiments, alternatives should be explored for future, tritium using experiments.

References

[1] G. Federici, R. Causey, P.L. Andrew, C.H. Wu, Fus. Eng. Des. 28 (1995) 136.
[2] G. Federici, D. Holland, G. Janeschitz, C.H. Wu, J. Nucl. Mater. 241–243 (1997) 260.
[3] G. Federici, R. Anderl, J.N. Brooks, R. Causey, J.P. Coad, D. Cowgill, R. Doerner, A.A. Haasz, G. Longhurst, S. Luckhardt, D. Mueller, A. Peacock, M. Pick, C. Skinner, W. Wampler, K. Wilson, C. Wong, C. Wu, D. Youchison, Fus. Eng. Des. 39 & 40 (1998) 445.
[4] G. Federici, R. Anderl, P. Andrew, J.N. Brooks, R.A. Causey, J.P. Coad, D. Cowgill, R.P. Doerner, A.A. Haasz, G. Janeschitz, W. Jacob, G.R. Longhurst, R. Nygren, A. Peacock, M.A. Pick, V. Philipps, J. Roth, C.H. Skinner, W.R. Wampler, J. Nucl. Mater. 266–269 (1998) 14.
[5] F. Waelbroeck, J. Winter, P. Wienhold, J. Nucl. Mater. 103–104 (1981) 471.
[6] F. Waelbroeck, P. Wienhold, J. Winter, J. Nucl. Mater. 111 & 112 (1982) 185.
[7] J. Winter, F.G. Waelbroeck, P. Wienhold, E. Rota, T. Banno, J. Vac. Sci. Technol. A 2 (2) (1984) 679.
[8] J. Ehrenberg, V. Philipps, L. de Kock, R.A. Causey, W.L. Hsu, J. Nucl. Mater. 176 & 177 (1990) 226.
[9] V. Philipps, J. Ehrenberg, J. Vac. Sci. Technol. A 11 (2) (1993) 437.
[10] J. Winter, J. Vac. Sci. Technol. A 5 (4) (1987) 2286.
[11] J. Ehrenberg, Hydrogen and helium recycling in tokamaks with carbon walls, Tech. Rep. JET-P(88)57, JET Joint Undertaking, 1988.
[12] R. Sartori, G. Saibene, D.H.J. Goodall, E. Usselmann, P. Coad, D. Holland, J. Nucl. Mater. 176 & 177 (1990) 624.
[13] P. Andrew, M. Pick, J. Nucl. Mater. 220–222 (1995) 601.
[14] K.L. Wilson, R. Bastasz, R.A. Causey, D.K. Brice, B.L. Doyle, W.R. Wampler, W. Möller, B.M.U. Scherzer, T. Tanabe, Trapping, detrapping and release of implanted hydrogen isotopes, in: Atomic and Plasma–Material Interaction Data for Fusion, Supplement to the Journal Nuclear Fusion, IAEA, Vienna, 1991, p. 31.
[15] G. Staudenmaier, J. Roth, R. Behrisch, J. Bohdansky, W. Eckstein, P. Staib, S. Matteson, S.K. Erents, J. Nucl. Mater. 84 (1979) 149.
[16] M. Braun, B. Emmoth, J. Nucl. Mater. 128 & 129 (1984) 657.
[17] M. Mayer, M. Balden, R. Behrisch, J. Nucl. Mater. 252 (1998) 55.
[18] A.A. Haasz, J.W. Davis, J. Nucl. Mater. 209 (1994) 155.
[19] A.A. Haasz, J.W. Davis, J. Nucl. Mater. 232 (1996) 219.
[20] M. Mayer, R. Behrisch, H. Plank, J. Roth, G. Dollinger, C.M. Frey, J. Nucl. Mater. 230 (1996) 67.
[21] M. Mayer, J. Nucl. Mater. 240 (1997) 164.
[22] J. Roth, B.M.U. Scherzer, R.S. Blewer, D.K. Brice, S.T. Picraux, W.R. Wampler, J. Nucl. Mater. 93 & 94 (1980) 601.
[23] W. Möller, B.M.U. Scherzer, J. Appl. Phys. 64 (10) (1988) 4860.
[24] M. Mayer, V. Philipps, H.G. Esser, P. Wienhold, M. Rubel, Wall pumping and hydrogen recycling in TEXTOR 94, in: Proceedings of the NATO Advanced Research Workshop on Hydrogen Recycle at Plasma Facing Materials, St. Petersburg, Russia, in print.
[25] T. Denner, K.H. Finken, G. Mank, N. Noda, Nucl. Fus. 39 (1999) 83.
[26] M. Rubel, P. Wienhold, D. Hildebrandt, J. Nucl. Mater., these proceedings.
[27] J.P. Coad, P.L. Andrew, A.T. Peacock, Physica Scripta T 81 (1999) 7.
[28] M. Mayer, R. Behrisch, P. Andrew, A.T. Peacock, J. Nucl. Mater. 241–243 (1997) 469.
[29] H. Verbeek, J. Stober, D.P. Coster, W. Eckstein, R. Schneider, Nucl. Fus. 38 (1998) 1789.
[30] J. von Seggern, M. Mayer, M. Rubel, H.G. Esser, V. Philipps, J. Nucl. Mater., these proceedings.
[31] P. Wienhold, H.G. Esser, D. Hildebrandt, A. Kirschner, M. Mayer, V. Philipps, M. Rubel, J. Nucl. Mater., these proceedings.
[32] J. Boedo, D. Gray, L. Chousal, R. Conn, B. Hiller, K.H. Finken, Rev. Sci. Instr. 69 (7) (1998) 2663.
[33] J. von Seggern, M. Rubel, P. Karduck, V. Philipps, H.G. Esser, P. Wienhold, Physica Scripta T 81 (1999) 31.
[34] P. Wienhold, H.G. Esser, D. Hildebrandt, A. Kirschner, K. Ohya, V. Philipps, M. Rubel, J. von Seggern, Physica Scripta T 81 (1999) 19.
[35] P. Wienhold, F. Waelbroeck, H. Bergsåker, J. Winter, H.G. Esser, J. Nucl. Mater. 162–164 (1989) 369.
[36] P. Wienhold, J. von Seggern, H.G. Esser, J. Winter, H. Bergsåker, M. Rubel, I. Gudowska, B. Emmoth, J. Nucl. Mater. 176 & 177 (1990) 150.

[37] M. Rubel, J. von Seggern, P. Karduck, V. Philipps, A. Vevecka-Priftaj, J. Nucl. Mater. 266–269 (1999) 1185.
[38] A. von Keudell, C. Hopf, T. Schwarz-Selinger, W. Jacob, Nucl. Fus. 39 (10) (1999) 1451.
[39] C. Hopf, T. Schwarz-Selinger, W. Jacob, A. von Keudell, J. Appl. Phys. 87 (6) (2000) 2719.
[40] M. Mayer, R. Behrisch, V. Prozesky, P. Andrew, A.T. Peacock, Surface layer composition of the JET vessel walls, material transport and hydrogen trapping in the vessel walls, in: 22nd EPS Conference on Controlled Fusion and Plasma Physics, Europhysics Conference Abstracts, vol. 19C, 1995, p. 301.
[41] P. Andrew, D. Brennan, J.P. Coad, J. Ehrenberg, M. Gadeberg, A. Gibson, M. Groth, J. How, O.N. Jarvis, H. Jensen, R. Lsser, F. Marcus, R. Monk, P. Morgan, J. Orchard, A. Peacock, R. Pearce, M. Pick, A. Rossi, B. Schunke, M. Stamp, M. von Hellermann, D.L. Hillis, J. Hogan, J. Nucl. Mater. 266–269 (1999) 153.
[42] P. Andrew, P.D. Brennan, J.P. Coad, J. Ehrenberg, M. Gadeberg, A. Gibson, D.L. Hillis, J. How, O.N. Jarvis, H. Jensen, R. Lässer, F. Marcus, R. Monk, P. Morgan, J. Orchard, A. Peacock, R. Pearce, M. Pick, A. Rossi, P. Schild, B. Schunke, D. Stork, Fus. Eng. Des. 47 (1999) 233.
[43] M. Mayer, R. Behrisch, K. Plamann, P. Coad, P. Andrew, A.T. Peacock, J. Nucl. Mater. 266–269 (1999) 604.
[44] M. Mayer, R. Behrisch, P. Andrew, P. Coad, A.T. Peacock, Physica Scripta T 81 (1999) 13.
[45] J.P. Coad, J. Nucl. Mater. 226 (1995) 156.
[46] J.P. Coad, M. Rubel, C.H. Wu, J. Nucl. Mater. 241–243 (1997) 408.
[47] J.P. Coad, J.D. Elder, S.K. Erents, G.F. Matthews, R-D. Penzhorn, P.C. Stangeby, J. Nucl. Mater., these Proceedings.
[48] R.-D. Penzhorn, N. Bekris, U. Berndt, P. Coad, Z. Helmut, N. Walter, presented at the 14th Int. Conf. on Plasma–Surface Interactions in Controlled Fusion Devices, Rosenheim, May 2000.
[49] H. Maier, K. Krieger, A. Tabasso, S. Lindig, V. Rohde, J. Roth, The ASDEX Upgrade Team, Deuterium inventories in different divertor configurations of ASDEX Upgrade, in: 26th EPS Conference on Controlled Fusion and Plasma Physics, Europhysics Conference Abstracts, vol. 23J, 1999, p. 1509.